(7) Lahti, P. M.; Modarelli, D. A.; Denton III, F. R.; Lenz, R. W.; Karasz, F. E. *J. Am. Chem. Soc.* **1988**, *110*, 7259.

(8) (a) Wessling, R. A.; Zimmerman, R. G. U. S. Patents 3401152 and 3404132, 1968; U.S. Patent 3532643, 1970; U.S. Patent 3705677, 1972. (b) Wessling, R. A. *J. Polym. Chem., Polym. Symp.* **1985**, *72*, 55.

(9) For a detailed review see: *Water-soluble Synthetic Polymers*; CRC Press: Boca Raton, FL, 1984.

(10) Han, C. C.; Jen, K. Y.; Elsenbaumer, R. L. *Proc. Int. Conf. Synth. Met.*, Santa Fe, NM; *Synth. Met.* **1989**, *30*, 123.

Registry No. **1**, 118943-21-8; **2**, 125714-79-6; **3**, 118943-23-0; **4**, 118943-24-1; **5**, 118943-25-2; **6**, 118943-26-3; **7**, 125714-80-9; **7** (homopolymer), 125714-83-2; **7** (SRU), 125714-84-3; **10**, 125714-85-4; **11**, 125714-86-5; **12**·Na, 125714-87-6; 4-methoxyphenol, 150-76-5; 3-chloropropanol, 627-30-5; methanesulfonyl chloride, 124-63-0; tetrahydrothiophene, 110-01-0.

Water-Soluble Copolymers. 30. Effects of Molecular Structure on Drag Reduction Efficiency

Charles L. McCormick,* Roger D. Hester, Sarah E. Morgan, and Abbas M. Safieddine

Department of Polymer Science, University of Southern Mississippi, Hattiesburg, Mississippi 39406-0076. *Received August 18, 1988; Revised Manuscript Received October 18, 1989*

ABSTRACT: Four series of high molecular weight, water-soluble acrylamide copolymers with specific compositions have been synthesized, characterized, and tested for drag reduction effectiveness. The comonomers sodium acrylate, sodium 2-(acrylamido)-2-methylpropanesulfonate, sodium 3-(acrylamido)-3-methylbutanoate, and diacetone acrylamide were utilized in appropriate molar ratios to provide tailored structures with varying degrees of hydrophobicity, ionic character, and propensity to form inter- or intramolecular associations. Drag reduction properties were measured in a modified rotating disk and a tube flow apparatus. A simple method of analyzing drag reduction performance was developed on the basis of hydrodynamic volume fraction normalization. This method allows comparison of diverse polymer types by efficiency curve superimposition utilizing an empirical shift factor. Drag reduction data were also analyzed by several conventional methods. Results demonstrate the dependence of drag reduction effectiveness on polymer structure as well as the importance of polymer–solvent interactions. Structure-performance analysis suggests that predictive theoretical models might be improved by inclusion of parameters reflective of solvent and associative interactions as well as hydrodynamic volume.

Introduction

It has been known for a number of years that certain additives can reduce energy loss due to friction in turbulent flow.[1] Drag reducing additives include low concentrations of high molecular weight polymers, micellar systems, and suspensions of fibers or other solids.[2] A large number of possible commercial applications for drag reduction (DR) have been the impetus for continued research in this area.[3] Despite the abundance of theoretical, experimental, and practical studies of the phenomenon that have appeared in the literature, many unanswered questions remain and no comprehensive, universally accepted model exists that explains the drag reduction mechanism.[4,5] In particular, the role of polymer microstructure and solvent interactions is not clear.

It is generally thought that macromolecular extension is involved in polymeric drag reduction.[6] Polymer molecules are thought to be elongated by shear forces in the turbulent flow regime. There is disagreement, however, as to whether the friction reduction results from an increased elongational viscosity or from an alteration of the energy balances in turbulent flow.[7,8]

Many researchers accept the proposal put forth by Lumley[9-11] which suggests that a fluid layer of substantially increased viscosity is present in the turbulent flow regime near the wall due to polymer elongation. In the layer of increased viscosity, damping of small dissipative eddies and reduced momentum transport from the buffer zone occur. In the viscous sublayer next to the wall, however, macromolecules are not greatly extended and viscosity is not increased appreciably above that for solvent alone.

Ryskin[12,13] recently developed a predictive theory incorporating Lumley's ideas and his own "yo-yo" model of polymer dynamics. The polymer effect on viscosity enhancement, ζ_{turb}, is given in eq 1,

$$\zeta_{turb} \simeq 0.05\alpha^3 N_A a^3 N^2 C/M_a \quad (1)$$

where N_A = Avogadro's number, M_a = molecular weight repeat unit, a = length of a repeat unit, α = ratio of chain length to that of a fully extended chain, C = polymer concentration, N = degree of polymerization. Ryskin relates ζ_{turb} to Virk's slope increment, δ_v (a measure of drag reduction effectiveness[14]), by eq 2. The δ value used

$$\delta = 2(1 + \zeta_{turb})^{1/2} - 2 \quad (2)$$

by Ryskin in eq 2 is half that of Virk's. Combination of eq 1 and 2 and rearrangement give eq 3, where molecular weight, M, is equal to M_aN. This relationship enables

$$[(\delta^2 + 4\delta)/2]^{1/3} = \alpha\{aN[N_A C/2M]^{1/3}\} \quad (3)$$

0024-9297/90/2223-2124$02.50/0

experimental determination of α, the ratio of polymer chain length to that of a fully extended chain. Ryskin's analysis indicated that α should have a value of ca. 0.2.

Walsh[15] developed a model based on the energy storage capability of polymer and associated solvent. In this model, polymer molecules interfere with small-scale vortices as they form near the wall. Macromolecules alter turbulence structure by weakening microdisturbances and preventing their growth. Walsh defined a dimensionless parameter, H, which describes the effect of polymer additives on the rate of diffusion of turbulence near the wall. Onset of turbulence is predicted at $H \simeq 0.01$ and maximum drag reduction at $H \simeq 1$.

$$H = (8CM[\eta]^2\tau_w)/RT \quad (4)$$

In eq 4, $[\eta]$, R, τ_w, and T are the polymer intrinsic viscosity, gas constant, wall shear stress, and temperature, respectively.

In Virk's "additive-burst" mechanism,[4] drag reducing additives interfere with the turbulent bursting process. Polymer molecules alter the turbulent energy balance by retarding transport of turbulent kinetic energy and axial momentum. Virk related DR effectiveness to polymer concentration in ppm, c, molecular weight, and degree of polymerization and suggested that a plot of reduced slope increment, $\Pi \equiv \delta_v/(c/M)^{1/2}$, as a function of degree of polymerization should yield a straight line.

de Gennes and Tabor[7,8] have recently presented an energy cascade theory of drag reduction. This scaling theory relates polymer length and deformation to turbulent energy dissipation. These authors suggest that friction reduction occurs primarily as a result of the elastic behavior of polymer molecules. Each coil behaves like a small spring which when deformed attains a certain elastic energy. When the elastic energy of the molecule is equal to the kinetic energy of the turbulent disturbance, the disturbance is suppressed.

This discussion of just a few of the many proposed models indicates the number of unsolved questions and the diversity of interpretations of the drag reduction phenomenon. Berman[5] has suggested multiple mechanisms that might operate simultaneously. Quantitative models have accurately predicted DR behavior of some water-soluble homopolymers (i.e., poly(ethylene oxide) and polyacrylamide[4,12,13,15]), but extensive analyses of polymers of widely differing structures and compositions have not been performed. In order to accurately assess the validity of the various models, further correlation with experimental data is required.

Many unanswered questions remain regarding the relationship between macromolecular structure and drag reduction performance.[16,17] Experimental studies have shown that a number of molecular parameters, including polymer molecular weight (MW), hydrodynamic volume, aggregation, chain stiffness, and polymer/solvent interactions,[18-34] affect drag reduction behavior. For example, drag reduction efficiency increases with increasing molecular weight and the high MW molecules in a MW distribution have the greatest effect on DR.[18-20] It is unclear, however, whether DR effectiveness is higher for polymers of higher MW primarily because of the increased chain length or the increased coil volume.[22] The quantitative relationships between drag reduction performance and other molecular parameters are also unclear.

The purpose of our continuing research is to systematically examine structure–drag reduction performance relationships of compositionally tailored water-soluble copolymers. Extensive studies of dilute solution properties including viscosity, phase behavior, hydrodynamic volume, and rheology of each copolymer type have been conducted in conjunction with these efforts. Comonomer models employed vary from negatively charged to hydrophobically modified acrylamide derivatives; these result in copolymers with a range of dilute solution properties.

Experimental Section

Polymer Synthesis. Acrylamide (AM) (from Aldrich Chemical Co.), diacetone acrylamide (DAAM) (from Polysciences, Inc.), and 2-(acrylamido)-2-methylpropanesulfonic acid (AMPSA) (from Polysciences, Inc.) were purified by three consecutive recrystallizations from acetone or methanol. Acrylic acid purchased from Aldrich Chemical Co. was purified via vacuum distillation. The monomer 3-(acrylamido)-3-methylbutanoic acid (AMBA) was synthesized via a Ritter reaction using commercial acrylonitrile and 3,3-dimethylacrylic acid following a previously published procedure.[35] AMBA was purified by recrystallization as described above. Charged monomers were placed in the sodium salt form prior to polymerization by equimolar addition of NaOH to aqueous monomer solution.

Polymerizations were performed in aqueous solution by using potassium persulfate free radical initiator at 30 °C under nitrogen atmosphere. Polymerization procedure is detailed elsewhere.[35-37] Reactions were terminated by precipitation in nonsolvent (acetone) before high conversion was attained (below 40% conversion) to prevent drift in copolymer composition. Polymers were purified by three cycles of dissolution in water followed by precipitation in acetone. Finally, the copolymers were isolated by freeze-drying from an aqueous solution (deionized water).

Polymer Characterization. Copolymer composition was determined from elemental analysis (M-H-W Laboratories, Phoenix, AZ) and ^{13}C NMR. Reactivity ratios were calculated statistically by both the Kelen–Tüdos and Fineman–Ross methods.[38,39]

Zero shear intrinsic viscosity, $[\eta]$, was obtained by using four-bulb shear dilution viscometers and/or a Contraves low shear 30 rheometer. Solution studies were performed in 0.514 M aqueous NaCl solution containing 0.01% NaN_3 as a biocide at 25 °C. Classical light scattering studies were performed by using a Chromatix KMX-6 low angle laser light scattering spectrophotometer utilizing a 2-mW He–Ne laser operating at 633 nm to obtain weight-average molecular weight, M_w. Specific refractive index increment, dn/dc, was determined from a Chromatix KMX-16 laser differential refractometer.

Drag Reduction Measurements. Polymer solutions were prepared by dissolving the required mass of polymer with 0.01% NaN_3 biocide in solvent in 1-L flasks by gentle room temperature stirring for 48 h. Solutions were then transferred to polypropylene tanks, diluted with solvent (deionized water or 0.514 M aqueous NaCl) to 20 L, and gently stirred for an additional 24 h before drag reduction measurements were made at 25 °C.

Polymeric solutions were tested for drag reduction performance in both a rotating disk and a tube flow apparatus. The first system consisted of a modified Haake, Model RV3, rheometer equipped with a rotating disk. The stainless-steel disk was 9 cm in radius, 2 mm in thickness, and was machined to ensure flatness and smoothness. The disk was centered in a chamber with the depth in the fluid being adjustable by changing the length of a stainless-steel shaft to which the disk was attached. The chamber was a Pyrex jar 305 mm in diameter by 457 mm in height with a capacity of 33.4 L.

The disk was driven by a variable speed motor. The motor drive and torque sensing unit are components from a Haake RV3 rotoviscometer. The torque applied to the rotating disk was determined by using the stress measuring head that was calibrated using the method described by the manufacturer.[40] The data acquisition system for recording the torque consisted of a Hewlett-Packard 41C calculator connected to an ADC 41 (Interface Instruments, Corvallis, OR) analog to digital interface. The experimental data, torque (τ_q) and disk angular velocity (ω), were converted to Reynolds number (Re) and friction

factor (f) using eq 5 and 6 which were developed for a disk of radius (R) rotating in an unbounded fluid of viscosity μ and density ρ.[41,42]

$$f = \tau_q/(\pi\rho\omega^2R^5) \quad (5)$$

$$\mathrm{Re} = \rho R^2\omega/\mu \quad (6)$$

The tube flow apparatus consisted of a smooth stainless-steel tube 102 cm in length, L, with a diameter, D, of 0.210 cm. This single pass testing system was driven by a high-pressure nitrogen gas source. Pressure taps were placed at 150 and 350 L/D downstream from the tube entrance to determine pressure drop. Pressure was measured by a Validyne DP 15 differential pressure transducer. Flow rate was monitored by a load cell with strain gauges connected to a Hewlett-Packard plotter where weight was plotted as a function of time. From measured pressure drop and flow rate, friction factor and Reynolds number were calculated.[41]

Results and Discussion

Copolymer Models. For the studies of the drag reduction phenomenon, copolymers were synthesized with particular structural attributes including specific placement of hydrophobic moieties and/or potential for strong inter- or intramolecular interactions (Table I). Acrylamide (AM) monomer is neutral and hydrophilic and polymerizes to a high molecular weight and large hydrodynamic volume in aqueous solutions. Sodium acrylate (NaA) is the negatively charged analogue to AM. Sodium 2-(acrylamido)-2-methylpropanesulfonate (NaAMPS) and sodium 3-(acrylamido)-3-methylbutanoate (NaAMB) are "anionic" comonomers with some hydrophobic character due to the geminal dimethyl groups (present to prevent hydrolysis of the amide linkage). PAM-*co*-NaAMPS and PAM-*co*-NaAMB copolymers are high molecular weight polyelectrolytes that have shown unusual tolerance to electrolytes (lack of phase separation) in aqueous solutions at elevated temperature.[43,44] These copolymers form intramolecular hydrogen-bonding interactions that result in stiffening of the chain at certain copolymer compositions.

The uncharged diacetone acrylamide (DAAM) monomer is more hydrophobic than acrylamide, to the extent that DAAM homopolymer is not water-soluble. When copolymerized with acrylamide, DAAM forms moderate molecular weight copolymers that show unusual intermolecular associations which promote viscosity. Quasielastic light scattering and membrane osmometry experiments have shown compositional effects on intermolecular bonding. A 20/80 DAAM/AM copolymer substantially increases viscosity in the presence of electrolytes such as NaCl (Table II).[45] These DAAM/AM copolymers are of considerable theoretical interest since cooperative bonding may dissociate under turbulent conditions to effect drag reduction. Under low shear the associations should recover.

Comonomer structures are shown in Table I. Measured zero shear intrinsic viscosities and weight-average molecular weights for selected copolymers are given in Table II. A homopolyacrylamide sample (PAM-4—synthesized under the same conditions used to prepare the copolymers) and a poly(ethylene oxide) sample (WSR-301—Union Carbide) are included for comparison with the copolymers.

For the PAM-*co*-NaAMB copolyelectrolytes, incorporation of small mole percentages of NaAMB comonomer (<35%) results in copolymers with molecular weights which are similar to that of the homopolyacrylamide standard (PAM-4), but intrinsic viscosities (measured in 0.514 M NaCl solutions) which are much higher. This viscosity enhancement results from stiffening of the chain due to intrapolymer interactions that occur at certain PAM-*co*-NaAMB copolymer compositions.[35] The homopolyelec-

Table I
Model Comonomers

comonomer	structure	properties
AM	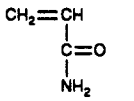	uncharged high MW homopolymer
NaA	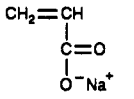	forms lower MW copolyelectrolytes poor salt tolerance
NaAMPS	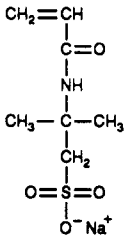	HMW copolyelectrolyte high salt tolerance large HDV in H_2O saline solution intramolecular hydrogen bonding stiffens chain, increases viscosity
NaAMB	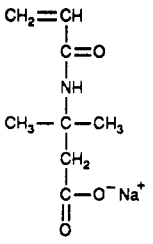	similar to NaAMPS but weaker acid; pH affects coil dimensions
DAAM	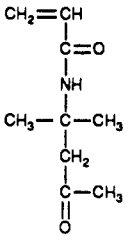	hydrophobic, uncharged hydrophobic inter- and intramolecular interactions intramolecular H-bonding associations in saline solution

Table II
Solution Properties of Selected Model Polymers in 0.514 M NaCl Solutions at 25 °C

sample name	mol % of comonomer in copolymer	$[\eta]$, dL/g[a]	$10^{-6}M_w$, g/mol[b]
	Homopolymers		
PEO WSR-301[c]	0	16	6.0
PAM-4	0	34	24
	Copolymers		
PAM-*co*-DAAM			
DAAM 15	17	18 (15)[d]	7.5 (3.5)
DAAM 20	20	16 (11)	6.9 (4.3)
DAAM 30	29	8.0 (6.2)	6.1 (5.9)
DAAM 35	35	3.4 (3.1)	3.6 (3.4)
PAM-*co*-NaA			
NaA 5	7.4	13	12
NaA 35	22	4.5	3.3
PAM-*co*-NaAMB			
NaAMB 10	10	47	28
NaAMB 40	34	50	22
NaAMB 100	100	8.4	3.6
PAM-*co*-NaAMPS			
NaAMPS 5	4.7	27	16
NaAMPS 10	9.2	44	18
NaAMPS 15	13	34	29
NaAMPS 20	18	38	27
NaAMPS 35	29	27	27
NaAMPS 100	100	8.0	6.8

[a] Zero shear intrinsic viscosity measured by low shear rheometry. [b] Weight-average molecular weight measured by low angle laser light scattering. [c] From Union Carbide. [d] Values in parentheses denote measurements in deionized water.

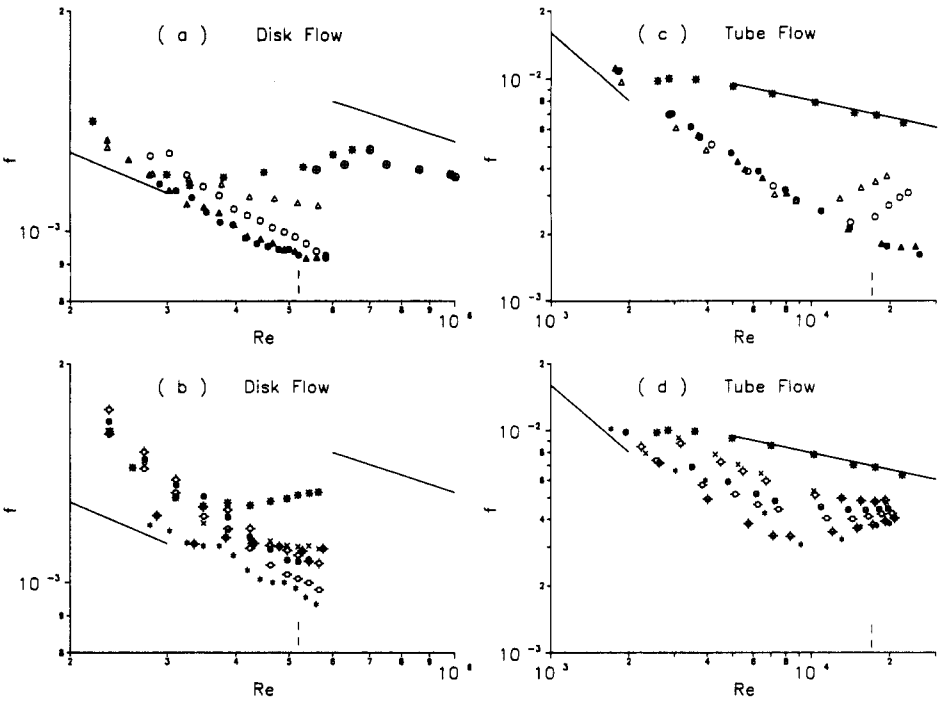

Figure 1. Typical friction factor vs Reynolds number plots for copolymers in 0.514 M NaCl solutions. Solid lines show theoretical predictions. (a) NaAMB 10, 3 ppm (○), 10 ppm (●); NaAMB 40, 3 ppm (△), 10 ppm (▲); DI water (✱); *n*-hexane (⊖). (b) DAAM 15, 3 ppm (×); DAAM 20, 3 ppm (◇); DAAM 30, 3 ppm (◒); DAAM 35, 3 ppm (⊙); PAM-4, 3 ppm (*); 0.514 M NaCl solvent (✱). (c) Same description as Figure 1a. (d) Same description as Figure 1b.

trolyte (NaAMB 100), on the other hand, is lower in M_w and $[\eta]$ than PAM-4. At all copolymer compositions the NaA copolyelectrolytes exhibited decreased $[\eta]$ and M_w in comparison to homopolyacrylamide.

For the hydrophobic DAAM copolymers, solution properties were measured in both aqueous and saline solutions. In general, measured apparent $[\eta]$ and apparent MW for these copolymers were greater in 0.514 M NaCl than in deionized water solution, reflecting their increased propensity to associate in the presence of added electrolytes. Dilute solution dimensions of these copolymers in deionized water were generally smaller than those of PAM-4.

Drag Reduction Studies. Rotating Disk Measurements. Typical friction factor vs Reynolds number plots for NaAMB copolymers tested in 0.514 M NaCl solution in the rotating disk and tube flow apparatus are shown in Figure 1. Polymer solution curves deviate from the solvent curve at a disk Reynold's number of approximately 300 000. This is the flow condition at which transition from laminar to turbulent flow is predicted to occur theoretically.[41] At disk Reynold's numbers greater than 300 000, addition of polymer serves to reduce the friction factor below that for solvent alone. The amount by which friction is reduced depends on polymer structure and concentration. Plots of this type were obtained for all copolymer models.

The solvent curve in Figure 1b exhibits a positive slope at high Reynolds numbers rather than the expected negative slope. This implies that the measurements taken may be in the transition zone between completely laminar flow and fully developed turbulence in which intermittent turbulent flow exists.[41] Due to limitations of the instrument, it was not possible to examine higher Reynolds numbers for aqueous solutions. However, higher Reynolds numbers could be generated for the lower viscosity, lower density solvent, *n*-hexane. In Figure 1a, composite f vs Re plots for water and *n*-hexane solvents are presented. The solid lines represent theoretical solvent behavior.[41] At a Reynolds number just above 750 000, the hexane curve changes slope indicating the beginning of the "fully turbulent" regime. Measurements were taken in aqueous solutions from just below this point up to a Reynolds number of 600 000.

Correlation with Tube Flow Measurements. Supplemental drag reduction measurements were performed in a tube flow apparatus to compare results from the rotating disk. The tube flow measurements allow a more direct assessment of the data correlation methods of Virk, Ryskin, and Walsh, as these were originally developed for tube flow. As shown by parts c and d, it was possible to generate a tube flow Reynolds number of 30 000, which is well above the laminar/turbulent transition of 2300.[41]

Parts a and c of Figure 1 show comparative behavior for NaAMB copolymers and parts b and d of Figure 1 the behavior of DAAM copolymers tested in both flow geometries. Although the magnitude of drag reduction at a given polymer concentration is greater in tube than in disk flow, relative DR trends measured as a function of polymer concentration and structure are the same. Similar trends were exhibited by the other copolymer models tested.

Many of the friction factor curves obtained for polymer solutions tested in the tube flow apparatus exhibit a change in slope at high Reynolds numbers. For example, at Reynolds numbers below 10 000, different NaAMB copolymer solutions showed identical behavior (Figure 1c). At a Reynolds number of ca. 10 000, the 3 ppm NaAMB 40 curve shows a change in slope, and at a slightly higher Re the 3 ppm NaAMB 10 curve changes slope, but the 10 ppm solution curve exhibits fairly constant, negative slope to Re $\simeq$ 30 000. This change in slope at high Re (and commensurate loss in DR effectiveness) for low polymer concentrations has often been observed in tube flow studies.[4,21,46,47] The slope change is a function of tube diameter, polymer molecular weight, and polymer concentration. Increases in diameter or polymer concentration shift the slope change to higher Reynolds numbers.

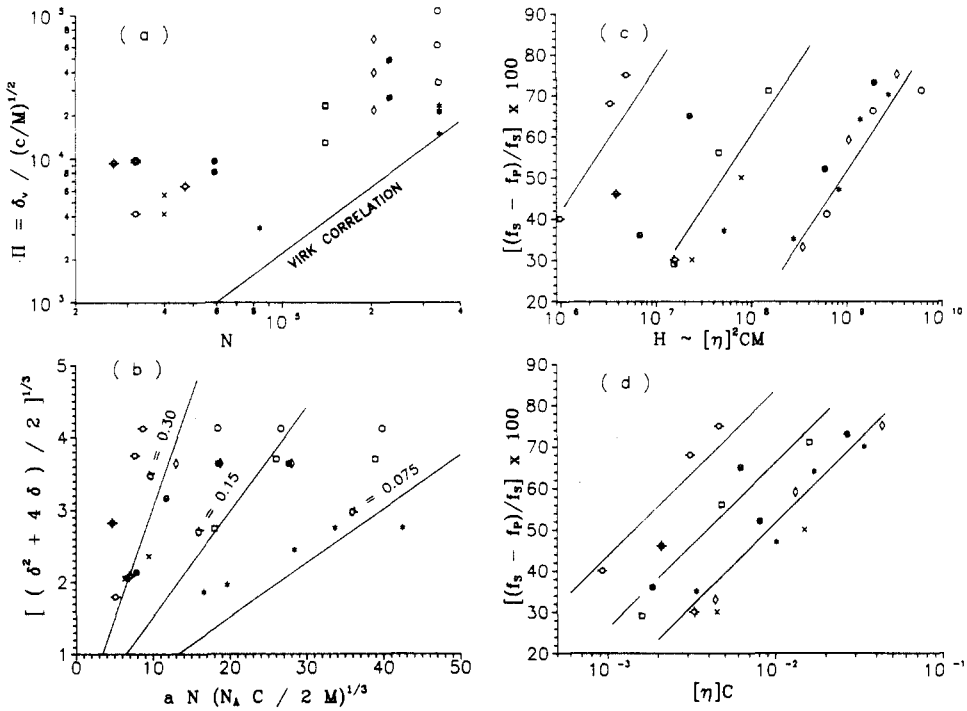

Figure 2. Comparison of drag reduction behavior of aqueous polymer solutions in tube flow at Re = 17 000 with literature methods. See Table III for symbol descriptions. (a) Virk plot of reduced slope increment as a function of the number of polymer chain links. (b) Ryskin plot as described by eq 3. (c) Walsh plot as suggested by eq 4. (d) Percent drag reduction vs polymer volume fraction parameter.

Berman[47] has suggested that the observed change in DR effectiveness occurs when the polymer chains are maximally extended. When Re is increased beyond this point, the polymer molecule can no longer respond to the increasing shear stresses and DR effectiveness decreases. As polymer concentration is increased, the Reynolds number at which all chains are maximally extended also increases. At some concentration, coil overlap will occur before the chains are fully extended. When this concentration is reached, the change in slope disappears.

The slope change observed in these studies apparently is not the "retro-onset" described by Virk for rigid-rod polymers.[4] The slope change seen here occurs for random coiling molecules like poly(ethylene oxide) and polyelectrolytes in saline solution. However, the chain stiffening intramolecular interactions present in the PAM-*co*-NaAMB copolymers may partially control the shape of the NaAMB curves.

For the ultrahigh molecular weight polyelectrolytes NaAMPS and NaAMB, differences in friction reduction behavior in tube flow at different polymer concentrations are exhibited only at high Reynolds numbers. At tube flow Reynolds numbers below the observed slope change, all polymer concentrations yield a single curve, but at higher Reynolds numbers relative drag reduction trends are identical with those seen in the rotating disk measurements (compare parts a and b of Figure 1). This interesting observation suggests that the rotating disk apparatus (at Reynolds numbers just beyond the laminar/turbulent transition) is quite sensitive to differences in polymeric drag reduction behavior.

Data Analysis Methods. Correlation with Literature Methods. In order to assess structure/drag reduction interrelationships, we examined several methods of data analysis discussed in the introduction. The number of well-characterized, structurally tailored molecules prepared in our laboratories lend themselves particularly to study the molecular parameters proposed in theoretical DR models.

Slope increments were obtained from initial slopes of Prandtl–von Karman plots[41] generated for the copolymer solutions tested in tube flow. We attempted to plot reduced slope increment as a function of degree of polymerization. Virk[4] reported that this type of plot yielded a straight line for flexible polymers with similar backbone linkages. Such a plot, however, exhibits a large amount of scatter (Figure 2a) for our copolymer models in which chain stiffening and viscosity enhancing intra- and/or intermolecular interactions are present.

A plot of the DR data with respect to Ryskin's proposed molecular model (eq 3) is shown in Figure 2b. Ryskin found that when the value of α (ratio of chain length to that of the fully extended chain) was adjusted, experimental DR data for PEO and PAM correlated well with his model. For our copolymer models, the values of α varied from 0.08 to 0.30. This variability suggests that α does not assume a constant value of ca. 0.2 as proposed by Ryskin.

In Figure 2c, a plot of percent drag reduction (% DR) as a function of the Walsh Parameter, H, is shown. Percent drag reduction is defined by

$$\% \text{ DR} \equiv [(f_s - f_p)/f_s] \times 100 \qquad (7)$$

where f_s and f_p are the friction factors for solvent and polymer solution, respectively. In general, % DR increases with increasing H up to a limiting maximum. Again, there is a large amount of scatter when different copolymer types are plotted together. However, as illustrated by the solid lines on the plot, correlation is observed for single copolymer types.

Both the Ryskin and Walsh analyses contain the dimensionless parameter $[\eta]C$, which is related to polymer volume fraction. This parameter is often used to compare solution properties of diverse polymer types. Hydrodynamic volume is a function of chemical structure, chain length, and interactions between polymer segments or polymer and solvent.

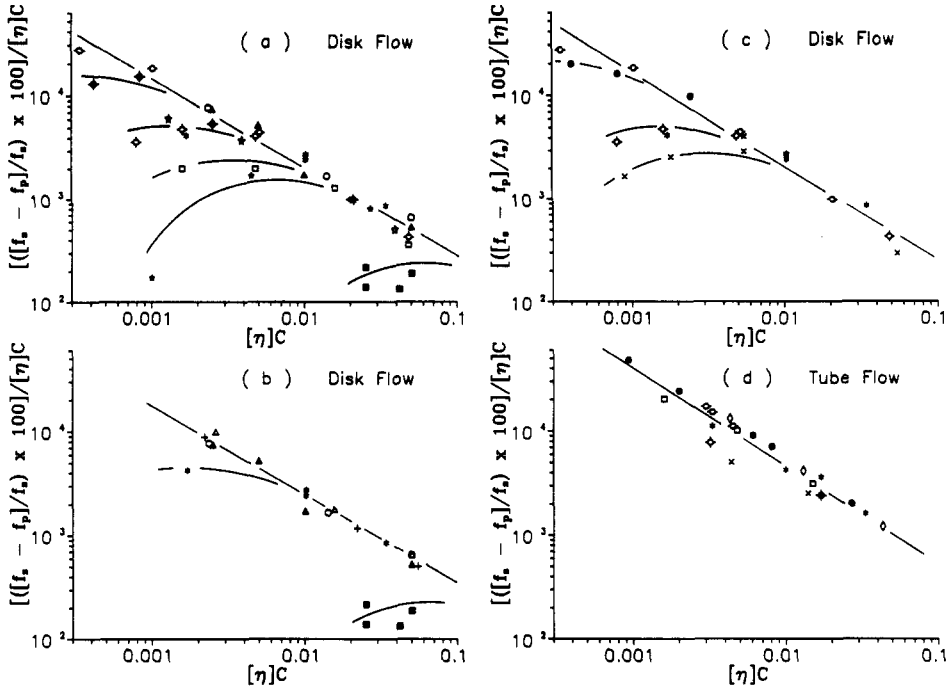

Figure 3. Drag reduction efficiency vs polymer volume fraction. See Table III for symbol descriptions. (a) Copolymer solutions in 0.514 M NaCl solvent tested in disk flow at Re = 520 000. (b) NaAMB copolymer solutions in 0.514 M NaCl solvent tested in disk flow at Re = 520 000. (c) DAAM copolymer solutions in 0.514 M NaCl solvent tested in disk flow at Re = 520 000. (d) Copolymer solutions tested in deionized water with tube flow at Re = 17 000.

Encouraged by results from Ryskin and Walsh type analyses, we first plotted % DR vs $[\eta]C$. Separate curves are obtained for particular structural types (Figure 2d). These correlations further illustrate the importance of polymer chemical structure, in addition to the effects of polymer coil dimensions, in determining drag reduction performance.

Volume Fraction Normalization. We have developed further normalization procedures that allow facile comparison of polymer types despite differences in degrees of polymerization and concentration. Such procedures are necessary for comparing copolymer performance and optimizing molecular design. We have obtained a measure of relative drag reduction efficiency at a given polymer volume fraction by normalizing % DR for $[\eta]C$. Figure 3 is a plot of DR efficiency (% DR/$[\eta]C$) as a function of $[\eta]C$ for selected copolymer models tested in the tube flow and rotating disk apparatus. The superimposed lines with a slope of negative one represent the maximum drag reduction envelope.

All of the copolymers tested in disk flow reach this envelope at some concentration (C_{max}), but the value of $[\eta]C$ that provides maximum DR varies with copolymer structure and composition (Figure 3a). At concentrations below C_{max}, DR efficiency can be improved by increasing polymer concentration. At concentrations above C_{max}, DR cannot be improved and further addition of polymer decreases efficiency. It should be noted that all copolymer solutions tested were in the dilute solution regime ($[\eta]C \ll 1$) and that $[\eta]$ values are those at zero shear. It is possible that apparent intrinsic viscosities measured at shear rates approximating those generated in the drag reduction testing systems might yield even better correlation.

Drag Reduction Studies of Tailored Models. The most effective drag reducers in disk flow are the polymers that yield the greatest DR efficiency (% DR/$[\eta]C$) at the lowest volume fractions. Thus, for our models the DAAM copolymers in disk flow are the most efficient, the uncharged homopolymers (PAM and PEO) yield moderate values, and the homopolyelectrolytes in this study are the least efficient. These trends may be seen more clearly when the copolymer types are examined individually.

Figure 3b shows DR efficiency curves for the NaAMB copolyelectrolytes in 0.514 M NaCl. The copolyelectrolytes with low mole percentages of charged comonomer exhibit similar, high efficiency curves, while the copolymers of higher charge content show reduced efficiency. The NaAMB homopolymer is much less efficient than the copolymers containing less than 35 mol % comonomer. Relative DR efficiency correlates with hydrodynamic volume for these copolyelectrolyte models. The most highly expanded copolymers in saline solution are those containing low mole percentages of charged groups, as evidenced by their high values of intrinsic viscosity (Table II). DR efficiency may also be related to increased chain stiffness from charge–charge repulsions and intramolecular hydrogen bonding that can persist even at high salt concentration in these copolymers.[35,43]

Figure 3c is a plot of the DR efficiency of the DAAM copolymers. For this series, efficiency increases with increasing content of the relatively hydrophobic DAAM comonomer. Note that the hydrodynamic volumes as measured by intrinsic viscosities and molecular weights decrease. Solvent ordering in the vicinity of hydrophobic moieties on the polymer chain[48-50] and associative interactions in dilute solution may contribute to the DR performance of the DAAM copolymers. The effects of solvent nature on DR performance will be discussed in more detail in the subsequent publication in this series. It is also interesting to note that all DAAM copolymers except DAAM 15 show increased efficiency in comparison to PAM-4, even though apparent molecular weights and intrinsic viscosities measured under low shear conditions are much smaller than those of PAM-4.

Figure 3d shows the DR efficiency of copolymer models tested in the tube flow apparatus. Relative trends are similar to those shown in disk flow (Figure 3a). The DAAM copolymers with high hydrophobic content yield

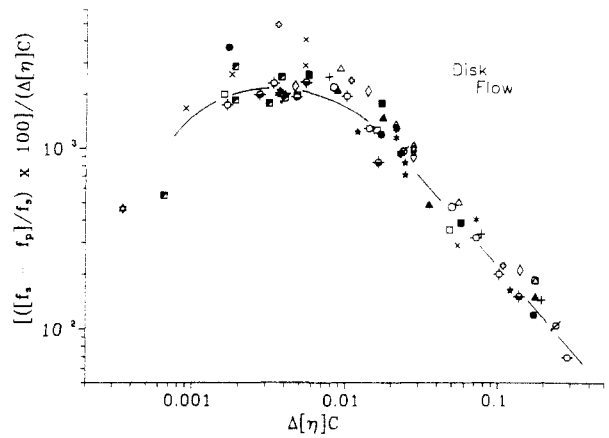

Figure 4. Polymer solution drag reduction efficiency vs polymer volume fraction employing shift factors. See Table III for symbol descriptions and shift factor information. Disk flow measurements were made at Re = 520 000.

Table III
Symbol Table and Polymer Shift Factors

polymer/solvent	symbol	shift factors in disk flow
solvents		
DI water	✳	
0.514 M NaCl	✳	
n-hexane	⊕	
homopolymers		
PEO WSR-301	□	1.0
PAM-4	*	2.0
copolymers		
DAAM 15	×	1.3
DAAM 20	◇	2.2
DAAM 25	◆	6.5
DAAM 30	●	8.0
DAAM 35	◇	10.0
NaA5	☆	3.0
NaA 10	★	3.0
NaA 20	✦	8.0
NaA 35	✡	0.35
NaAMB 5	+	3.5
NaAMB 10	○	3.5
NaAMB 25	△	3.5
NaAMB 40	▲	3.5
NaAMB 100	◩	0.075
NaAMPS 5	■	2.1
NaAMPS 10	◊	2.1
NaAMPS 15	✣	2.1
NaAMPS 20	⌀	2.1
NaAMPS 35	●	2.1
NaAMPS 100	⌀	0.09

highest efficiency at low volume fraction; PEO WSR-301 and PAM-4 give moderate values.

Further Normalization Methods. It was found that a shift factor, Δ, could be employed to allow all polymer disk flow data to fall on a single efficiency curve. The PEO WSR-301 curve was chosen as a standard to which all other curves were adjusted; thus Δ for PEO is equal to one. The abscissa values were multiplied by Δ and ordinate values divided by Δ to produce the single curve shown in Figure 4. A shift factor greater than one indicates a higher efficiency in frictional reduction than that exhibited for PEO, and Δ less than one denotes decreased efficiency. Table III lists Δ values for all polymer solutions tested in disk flow. Shift factors range over 2 orders of magnitude. DAAM 35 gives the greatest value of Δ, and the homopolyelectrolytes exhibit the lowest. The numerical value of Δ is apparently related to molecular properties that affect DR performance.

Our reported method of data reduction is relatively simple and requires only the knowledge of polymer intrinsic viscosity and concentration. It may be used to analyze DR data obtained from a variety of testing geometries. Interpretation of the curves is also simple; relative drag reduction efficiency of different copolymer types is readily distinguished. Use of the shift factor provides a numerical gauge of relative DR performance. As strongly implied by examination of the polymer models in this work, Δ may be a function of polymer molecular weight, ability to associate, chain flexibility, and/or polymer/solvent interactions between copolymers.

Conclusions

Several series of water-soluble copolymers were synthesized with ranges of copolymer compositions to provide macromolecules with varying degrees of hydrophobicity, charge character, and propensity to form inter- or intramolecular associations. Copolymers were thoroughly characterized for composition, microstructure, and low shear aqueous solution behavior. Drag reduction effectiveness was evaluated by using both rotating disk flow and tube flow apparatus. A relatively simple empirical method of analyzing drag reduction performance has been developed which yields a drag reduction efficiency plot related to hydrodynamic volume of polymer in solution. A clear dependence of drag reduction effectiveness on copolymer composition was observed. Slight changes in polymer chemical structure drastically affect drag reduction performance. Associating copolymers yield the highest drag reduction efficiency, and hydrophobic content is related to drag reduction performance rather than to hydrodynamic volume. For the copolyelectrolytes tested, maximizing hydrodynamic volume optimizes drag reduction efficiency. Low incorporation (5–30%) of charged comonomer gives high molecular weight, high intrinsic viscosity copolymers with greatest drag reduction. Several of the copolymers synthesized exhibit more efficient drag reduction performance than poly(ethylene oxide) or polyacrylamide standards. Examination of the data by proposed theoretical models indicates that predictions based solely on polymer coil dimensions and concentration cannot correctly predict drag reduction performance for different polymer types. A truly predictive model must also incorporate the effects of molecular parameters such as associations, polymer/solvent interactions, and chain stiffness.

A subsequent publication in this series involving these copolymer models will examine in more detail the individual effects of polymer molecular weight, hydrodynamic volume, solvent nature, and associations on drag reduction performance. Studies analyzing the effects of molecular weight distribution and the drag reduction behavior of other copolymer types are presently underway in our laboratories. It is our hope that these and similar studies in other laboratories will provide information about the specific role of macromolecules in the drag reduction mechanism.

Acknowledgment. Partial financial support from the Defense Advanced Research Projects Agency, the Office of Naval Research, and the Mississippi–Alabama Sea Grant Consortium is gratefully acknowledged.

References and Notes

(1) Toms, B. A. *Proceedings International Congress on Rheology*; North Holland Publishing Co.: Amsterdam, 1949; Vol. II, p 135.

(2) Hoyt, J. W. *Trans. ASME* **1972**, *94*, 258.
(3) Sellin, R. H. J.; Hoyt, J. W.; Scrivener, O. *J. Hydraulic Res.* **1982**, *20* (1), 29.
(4) Virk, P. S. In *Biotechnology of Marine Polysaccharides*; Colwell, R., Pariser, E. R., Sinskey, A. J., Eds.; Hemisphere: Washington, 1985; p 149.
(5) Berman, N. S. In *The Influence of Polymer Additives on Velocity and Temperature Fields*; Gampert, B., Ed.; Springer-Verlag: Berlin, 1985; p 293.
(6) Hoyt, J. W. Drag Reduction. In *Encyclopedia of Polymer Science and Engineering*; Wiley-Interscience: New York, 1986; Vol. 5, p 129.
(7) de Gennes, P.-G. *Physica* **1986**, *140A*, 9.
(8) Tabor, M.; de Gennes, P. G. *Europhys. Lett.* **1986**, *2* (7), 519.
(9) Lumley, J. L. In *Annual Reviews of Fluid Mechanics, 1*; Annual Reviews, Inc.: Palo Alto, CA, 1969; p 367.
(10) Lumley, J. L. *J. Polym. Sci., Macromol. Rev.* **1973**, *7*, 263.
(11) Lumley, J. L.; Kubo, I. In *The Influence of Polymer Additives on Velocity and Temperature Fields*; Gampert, B., Ed.; Springer-Verlag: Berlin, 1985; p 3.
(12) Ryskin, G. *Phys. Rev. Lett.* **1987**, *59* (18), 2059.
(13) Ryskin, G. *J. Fluid Mech.* **1987**, *178*, 423.
(14) Virk, P. S. *AIChE J.* **1975**, *21* (4), 625.
(15) Walsh, M. Ph.D. Thesis, California Inst. of Tech., 1967.
(16) Kulicke, W. M.; Klein, J. In *The Influence of Polymer Additives on Velocity and Temperature Fields*; Gampert, B., Ed.; Springer-Verlag: Berlin, 1985; p 43.
(17) Layec-Raphalen, M. N.; Layec, Y. In *The Influence of Polymer Additives on Velocity and Termpature Fields*; Gampert, B., Ed.; Springer-Verlag: Berlin, 1985; p 89.
(18) Berman, N. S. In *Annual Reviews of Fluid Mechanics, 10*, Annual Reviews Inc.: Palo Alto, CA, 1978; p 47.
(19) Liaw, G.-C.; Zakin, J. L.; Patterson, G. K. *AIChE J.* **1970**, *17* (2), 391.
(20) Gampert, B.; Wagner, P. In *The Influence of Polymer Additives on Velocity and Temperature Fields*; Gampert, B., Ed.; Springer-Verlag: Berlin, 1985; p 71.
(21) Kulicke, W.-M.; Grager, H. In *Proceedings of the Third International Conference on Drag Reduction*; Sellin, R. H. J., Moses, R. T., Eds.; IAHR: Bristol, England, 1984; Paper A.5.
(22) Matjukhov, A. P.; Mironov, B. P.; Anisimov, I. A. In *The Influence of Polymer Additives on Velocity and Temperature Fields*; Gampert, B., Ed.; Springer-Verlag: Berlin, 1985; p 107.
(23) Dunlop, E. H.; Cox, L. R. *Phys. Fluids* **1977**, *20* (10), S203.
(24) McCormick, C. L.; Hester, R. D.; Morgan, S. E.; Safieddine, A. M. *Polym. Mat. Sci. Eng.* **1987**, *57*, 840.
(25) Rochefort, S.; Middleman, S. *Polymer-Flow Interactions*, AIP Conference Proceedings; Yitzhak Rabin, Ed.; La Jolla, 1985; No. 137, p 117.
(26) Kowalik, R. M.; Duvdevani, I.; Peiffer, D. G.; Lundberg, R. D.; Kitano, K.; Schulz, D. N. *Non-Newtonian Fluid Mech.* **1987**, *24*, 1.
(27) Kim, O.-K.; Little, R. C.; Ting, R. Y. *AIChE Symp. Ser.* **1973**, *69*, 39.
(28) Kim, O.-K.; Long, T.; Brown, F. *Polym. Commun.* **1986**, *27*, 71.
(29) Kim, O.-K.; Choi, L. S.; Long, T. S.; Yoon, T. H. *Polym. Prepr. (Am. Chem. Soc., Div. Polym. Chem.)* *28* (2), 68.
(30) Kim, O.-K.; Long, T.; Choi, L.-S.; Yoon, T. H. *Proc. PMSE* **1987**, *57*, 835.
(31) Berman, N. S.; Berger, R. B.; Leis, J. R. *J. Rheol.* **1980**, *24* (5), 571.
(32) Patterson, R. L.; Little, R. C. *J. Colloid Interface Sci.* **1975**, *53*, 110.
(33) Parker, C. A.; Hedley, A. H. *JAPS* **1974**, *18*, 3403.
(34) Zakin, J. L.; Hunston, D. L. *J. Macromol. Sci. Phys.* **1980**, *B18* (4), 795.
(35) McCormick, C. L.; Blackmon, K. P. *J. Polym. Sci., Polym. Chem. Ed.* **1986**, *24*, 2635.
(36) McCormick, C. L.; Chen, G. S. *J. Polym. Sci., Polym. Chem. Ed.* **1982**, *20*, 817.
(37) McCormick, C. L.; Chen, G. S. *J. Polym. Sci., Polym. Chem. Ed.* **1984**, *22*, 3633.
(38) Kelen, T.; Tudos, F. J. *J. Macromol. Sci. Chem.* **1975**, *A9*, 1.
(39) Fineman, M.; Ross, S. *J. Polym. Sci.* **1950**, *5* (2), 259.
(40) Instruction Manual, Model Rotovisco RV3, Haake Instruments, Saddle Brook, NJ.
(41) Schlichting, H. *Boundary Layer Theory*; McGraw-Hill: New York, 1979, p 647.
(42) Bird, R. B.; Stewart, W. E.; Lightfoot, E. N. *Transport Phenomena*; Wiley; New York, 1960; p 181.
(43) McCormick, C. L.; Blackmon, K. P.; Elliott, D. L. *J. Polym. Sci., Polym. Chem. Ed.* **1986**, *24*, 2619.
(44) McCormick, C. L.; Elliott, D. L. *Macromolecules* **1986**, *19*, 542.
(45) McCormick, C. L.; Hutchinson, B. H.; Morgan, S. E. *Makromol Chem.* **1987**, *188*, 357.
(46) Sellin, R. H. J.; Loeffler, E. J. In *Second International Conference on Drag Reduction*; BHRA Fluid Eng: Cambridge, England, 1977; Paper C2.
(47) Berman, N. S. *Phys. Fluids* **1977**, *20* (5), 715.
(48) Jellinek, H. H. G. *Water Structure at the Water-Polymer Interface*; Plenum Press: New York, 1972.
(49) Tanford, C. *The Hydrophobic Effect, Formation of Micelles and Biological Membranes*; Wiley: New York, 1973.
(50) Hoy and Hoy (Union Carbide Corp.) U.S. Patent 4,209,605, 1980.

Registry No. PAM-*co*-DAAM, 25231-54-3; PAM-*co*-NaA, 25085-02-3; PAM-*co*-NaAMB, 100047-18-5; PAM-*co*-NaAMPS, 38193-60-1.